International Journal of Pharmaceutics 387 (2010) 103–109

Contents lists available at ScienceDirect

International Journal of Pharmaceutics

journal homepage: www.elsevier.com/locate/ijpharm

Possible reduction of effective thickness of intestinal unstirred water layer by particle drifting effect

Kiyohiko Sugano*

Global Research & Development, Sandwich Laboratories, Research Formulation, Pfizer Inc., CT13 9NJ, Sandwich, Kent, UK

ARTICLE INFO

Article history:
Received 23 September 2009
Received in revised form 3 December 2009
Accepted 4 December 2009
Available online 16 December 2009

Keywords:
Oral absorption
Particle size
Unstirred water layer
Permeability

ABSTRACT

According to the present theory of oral absorption, in the case of solubility limited absorption, the absorbed amount would not increase despite an increase in dose or a decrease in particle size. However, many experimental observations suggested that the absorbed amount was often increased (though sub-proportionally) as the dose strength increased. In addition, the particle size reduction was often effective to increase the absorbed amount even in the case of solubility limited absorption. Since an increase of the dose strength and a decrease of the particle size cause no or little change in solubility and the mean intestinal transit time, effective intestinal membrane permeability (P_{eff}) should have changed. The previous theory postulated that drug particles do not exist in the unstirred water layer (UWL) which is adjacent to the intestinal membrane. However, many reports suggested that nano- to micro-scale drug particles existed in the UWL. In this case, the *effective* thickness of the UWL (h_{eff}) could be smaller than the nominal thickness, resulting in an increase of P_{eff}. In the present study, h_{eff} was simply calculated assuming that the reduction of h_{eff} is in proportion to the surface area of drug particles in the UWL. When the particle drifting effect was taken into account, the discrepancy between the theoretical calculation and experimental observations was reduced. It was suggested that when the dose (mg)/particle diameter (μm) ratio exceeds 20, the particle drifting effect would become significant.

1. Introduction

Oral absorption simulation is anticipated to be a useful tool in drug discovery and development. Theoretical frameworks of oral absorption have been extensively investigated in the last two decades (Dressman and Fleisher, 1986; Haruta et al., 1998; Johnson, 2003; Sawamoto et al., 1997; Yu, 1999; Yu and Amidon, 1999). The previous theory resulted in a reasonable prediction of the fraction of a dose absorbed (*Fa*) when the dose strength (*Dose*) and the particle radius (r_p) were moderate (*Dose* < ca. 4–5 mg/kg, r_p > ca. 3 μm) (Sugano, 2009a, 2009d; Takano et al., 2008, 2006). According to the previous theory, the causes for incomplete oral absorption can be categorized into the permeability, dissolution rate and solubility limited cases (Sugano et al., 2007; Takano et al., 2008; Yu, 1999). In the solubility limited case, the previous theory suggested that the absorbed amount (X_{abs}) would not increase with the increase of the dose strength since the concentration in the intestinal fluid becomes saturated (Fig. 1) (Sugano et al., 2007; Takano et al., 2008; Yu, 1999). In addition, the previous theory suggested that particle size reduction increase X_{abs} in the case of dissolution rate limited absorption, however, not in the case of solubility limited absorption. However, these theoretical suggestions were inconsistent with experimental observations at higher dose strength and/or smaller particle size in many cases, for example efavirenz (FDA approval document for Sustiva). X_{abs} was often increased as dose increased (though the increase was sub-proportional to the dose) even at a high dose range. In addition, the increase of X_{abs} by a particle size reduction exceeded that predicted from the increase of the dissolution rate (Jinno et al., 2006; Liversidge and Cundy, 1995). The purpose of the present study was to investigate a hypothetic mechanism, "particle drifting into the unstirred water layer", which could possibly explain the discrepancy.

2. Theory

Previously, effective intestinal membrane permeability (P_{eff}) was tacitly assumed to be independent of *Dose* and r_p. We revisit this assumption in the following discussions.

According to the previous theory, in the case of solubility limited absorption, X_{abs} is basically determined by saturated solubility ($S_{dissolv}$), P_{eff}, the intestinal surface area (SA_{GI}, smooth tube based) and the saturated solubility duration time (T_{sat}) (Avdeef, 2006; Dressman et al., 1985; Johnson and Swindell, 1996; Oh et al., 1993). The main absorption site is usually the small intestine.

$$X_{abs} = SA_{GI} \cdot P_{eff} \cdot S_{dissolv} \cdot T_{sat} \quad (1)$$

* Tel.: +44 1304 644338.
E-mail address: Kiyohiko.Sugano@pfizer.com.

0378-5173/$ – see front matter © 2010 Elsevier B.V. All rights reserved.
doi:10.1016/j.ijpharm.2009.12.014

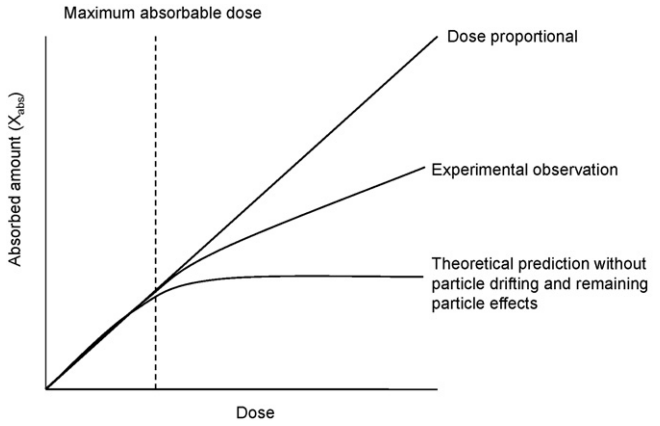

Fig. 1. Schematic presentation of the discrepancy between the previous theory and observations.

Therefore, in the case of solubility limited absorption, the previous theory suggested that an increase of the dose strength and a decrease of the particle size would cause no increase of X_{abs} if $S_{dissolv}$, P_{eff}, T_{sat} and SA_{GI} are independent of *Dose* and r_p (cf. in the case of dissolution rate limited absorption, *Dose* and r_p affect X_{abs}) (Sugano et al., 2007; Takano et al., 2008; Yu, 1999). $S_{dissolv}$ would not be affected by *Dose* and r_p unless the particle size is less than <100 nm. T_{sat} would be increased as the dose strength is increased since the remaining portion of the drug particles in the small intestine would be increased due to the distribution of the small intestine transit time (Yu and Amidon, 1998) and the saturated concentration would be maintained longer than the mean residual time (T_{si}) (residual particle effect (RPE)) (Sugano, 2009a, 2009c). However, this effect was not large enough to explain the discrepancy (discussed later). The change of SA_{GI} by the dispersion of drug particles along the small intestinal tract was factored into the RPE (Sugano, 2009b, 2009c). Therefore, by the process of elimination, it was suggested that P_{eff} should be significantly increased by both an increase of the dose strength and a decrease of the particle size.

The intestinal membrane permeation is a sequential process of the unstirred water layer (UWL) and epithelial membrane permeations. When time averaged, the UWL is a stagnant water layer which is adjacent to the intestinal wall and indistinctly separated from the well-stirred bulk fluid. In many cases of high lipophilicity compounds (octanol water distribution coefficient at pH 6.5 ($\log D_{pH6.5}$) > 1–2), the epithelial membrane permeation is rapid, and therefore, the UWL permeation becomes the rate limiting step (Martin, 1981; Obata et al., 2005; Sugano, 2009e). The previous theory tacitly postulated that drug particles would exist restrictedly in the well-stirred bulk fluid. In this case, the drug molecules dissolved in the bulk fluid would diffuse from the bulk fluid/UWL interface to the epithelial cell membrane (Fig. 2A).

2.1. Concept of particle drifting effect

However, many reports suggested that a significant portion of micrometer scale particles can drift into the UWL (Doyle-McCullough et al., 2007; Hodges et al., 1995; Limpanussorn et al., 1998; Norris et al., 1998; Smyth et al., 2008). The total thickness of the UWL (h_{totUWL}) is reported to be ca. 0.03 cm (a plicate surface based value. It is 0.01 cm when based on a smooth surface) (Fagerholm and Lennernaes, 1995; Lennernaes, 2007; Sugano, 2009a,c). The UWL consist of the mucus and aqueous boundary layers (the latter is called the Prantls boundary layer which is maintained solely by viscosity of water) (Fig. 2). The mucus layer is divided into two regions, the firmly adhered and loosely bound regions (Allen and Flemstroem, 2005; Atuma et al., 2001). The loosely bound mucus can be renewable by a fluid flow. Previously, it was found that a significant portion of micro-scale particles can drift into the loosely bound mucus region (Doyle-McCullough et al., 2007; Hodges et al., 1995; Limpanussorn et al., 1998; Norris et al., 1998; Smyth et al., 2008). In addition, a portion of particles smaller than <2–5 μm was found to permeate further into the firmly adhered mucus and reach the epithelial cell membrane (Desai et al., 1996; Doyle-McCullough et al., 2007; Florence, 1997; Gaumet et al., 2009; Moyes et al., 2007). Therefore, the effect of drug particles in the UWL which was neglected in the previously theory should be taken into account for P_{eff} calculation.

When drug particles drifted into the UWL, these particles could be a reservoir of a drug in the UWL and the drug particles would dissolve in the UWL. The dissolved drug molecules would diffuse

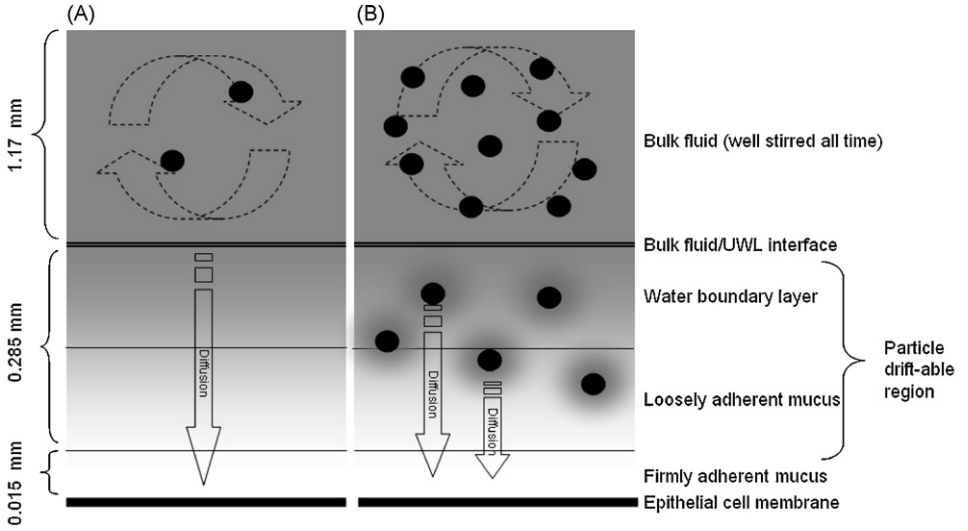

(A) Low dose. Drug molecules are supplied only from the bulk fluid/UWL interface.
(B) High dose. Drug molecules are supplied from both the particle surface in the UWL and the bulk fluid/UWL interface.

Fig. 2. Particle drifting effect. The grey gradient represents the concentration of dissolved drug molecules. (A) Without particle drifting into the UWL (B) with particle drifting into the UWL.

from the drug particles to the epithelial cell membrane (Fig. 2B). When the dose was increased and/or particle size was decreased, the number of drug particles in the UWL would be increased. This would increase the portion of the drug molecules diffusing from the drug particle in the UWL. Since the distance from the drug particle in the UWL to the epithelial cell membrane is smaller than that from the bulk fluid/UWL interface, when the drug particles exist in the UWL, the *effective* thickness of the UWL as the diffusion resistance (h_{eff}) becomes smaller.

2.2. Mathematical formula

The effective thickness of the UWL (h_{eff}) was simply calculated assuming that h_{eff} is in reciprocal to the surface area of drug particles in the UWL (SA_p).

2.2.1. Calculation of drug particle surface area in UWL

The surface area of drug particles in the UWL (SA_p) for poly dispersed particles can be expressed as,

$$SA_p = C_{pd} \cdot f_{UWL} \cdot \sum_i N_i \cdot 4\pi r_{p,i}^2 \quad (2)$$

where N_i is the number of drug particles in a particle size bin i, $r_{p,i}$ is the particle radius, f_{UWL} is the volume ratio of the total intestinal fluid and the particle drift-able region, and C_{pd} is the particle drifting coefficient (discussed later in detail). Log normal distribution with a standard distribution of 0.3 log unit was assumed for particle size distribution.

f_{UWL} can be estimated as,

$$f_{UWL} = \frac{h_{pd}}{h_{fluid}} = \frac{h_{pd}}{V_{GI}/SA_{UWL}} = \frac{h_{pd}}{V_{GI}/(PE \cdot SA_{GI})} = \frac{2 \cdot DF \cdot PE \cdot h_{pd}}{R_{GI}} \quad (3)$$

where h_{pd} is the thickness of the particle drift-able region (Fig. 2), h_{fluid} is the total thickness of the intestinal fluid on the UWL surface ($=V_{GI}/SA_{UWL}$), SA_{UWL} is the UWL surface area (the area of the bulk fluid/UWL interface) which is equal to the plicate surface area, and PE is the surface expansion by the plicate structure ($SA_{UWL} = SA_{GI} \cdot PE$). SA_{GI} is the intestinal tube surface area assuming a smooth surface. DF is the degree of flatness of the GI tube and R_{GI} is the radius of the GI tube (cf. *for cylindrical*, $SA_{GI}/V_{GI} = 2\pi R_{GI}/\pi R_{GI}^2 = 2/R_{GI}$ and $DF = 1$).

N_i can be calculated as,

$$N_i = \frac{f_i \cdot Dose}{(4\pi r_{p,i}^3/3) \cdot \rho} \quad (4)$$

where f_i is the fraction of a drug in a particle size bin i, ρ is the true density of a drug (set to 1.2 g/cm^3 in the present study). The ratio of the particle surface area in the particle drift-able region (SA_p) and the UWL surface area (SA_{UWL}) is then defined as,

$$R_{SA} = \frac{SA_p}{SA_{UWL}} \quad (5)$$

R_{SA} is the key parameter of this study, which determines the portion of drug molecules diffusing from the bulk fluid/UWL interface and drug particle surface in the UWL (cf. the concentrations at the particle surface and at the bulk fluid/UWL interface are both the saturated solubility).

Combining Eqs. (2)–(5),

$$R_{SA} = \frac{R_{GI} \cdot C_{pd} \cdot f_{UWL}}{2DF \cdot V_{GI} \cdot PE} \sum_i \frac{3 \cdot f_i \cdot Dose}{r_{p,i} \cdot \rho}$$

2.2.2. Calculation of effective UWL thickness

The difference between h_{totUWL} and the thickness of the firmly adhered mucus layer (h_{fam}) is defined as the thickness of the particle drift-able region (h_{pd}).

$$h_{pd} = h_{totUWL} - h_{fam} \quad (6)$$

When particles are evenly distributed in the particle drift-able region, by using the average vertical position of particles ($1/2\, h_{pd}$), the effective thickness of the intestinal UWL (h_{eff}) can be expressed as,

$$h_{eff} = h_{fam} + h_{pd} - \tfrac{1}{2} h_{pd} \cdot R_{SA}, \quad R_{SA} \le 1 \quad (7)$$

When the particles in the particle drift-able region is zero, R_{SA} is zero and $h_{eff} = h_{fam} + h_{pd} = h_{totUWL}$. Therefore, Eq. (7) connotes the previous theory. When the surface area of drug particles in the UWL equals the SA_{UWL}, $SA_p = SA_{UWL}$ and R_{SA} is 1, therefore $h_{eff} = h_{fam} + (1/2)\, h_{pd}$. When the drug particle surface area exceeds the UWL surface area (i.e., $SA_p > SA_{UWL}$, $R_{SA} > 1$), the effective thickness of the particle drifting area decreases in reciprocal to R_{SA}. Therefore,

$$h_{eff} = h_{afm} + \frac{1}{2} \cdot \frac{h_{pda}}{R_{SA}}, \quad R_{SA} > 1 \quad (8)$$

When taking a limit of R_{SA}, $h_{eff} = h_{fam}$, which is the minimum h_{eff}. These calculation schemes are the simple first approximation and the deviation may be factored into the fitting coefficient of C_{pd}.

2.2.3. Calculation of effective permeability

The effective UWL permeability (P_{UWL}) was calculated as previously reported (Sugano, 2009a,c).

$$P_{UWL} = \frac{D_{eff,UWL}}{h_{eff}} + P_{WC} \quad (9)$$

where $D_{eff,UWL}$ is the effective diffusion coefficient in the UWL, and P_{WC} is the UWL permeability coefficient by water conveyance. $D_{eff,UWL}$ is expressed as,

$$D_{eff,UWL} = D_{mono} \cdot f_{mono} + D_{bm} \cdot (1 - f_{mono}) \quad (10)$$

where D_{mono} is the diffusion coefficients of unbound monomer molecules, D_{bm} is the diffusion coefficient of bile micelle bound molecules in the UWL, and f_{mono} is the fraction of free monomer. f_{mono} can be calculated as the ratio of solubility in blank buffer (S_{blank}) and bile micelle media ($S_{dissolv}$) ($f_{mono} = S_{blank}/S_{dissolv}$). The fasted state and fed state simulated intestinal fluids (FaSSIF and FeSSIF) were used as bile micelle media (Galia et al., 1998; Glomme et al., 2006). D_{mono} was calculated from the molecular weight (MW) ($D_{mono} = 1.41 \times 10^{-4.113 - 0.4609 \times \log MW}$) (Avdeef, 2003). P_{eff} is expressed as (Amidon et al., 1982; Sugano, 2009a,c),

$$\frac{1}{P_{eff}} = \left(\frac{1}{P_{UWL}} + \frac{1}{f_{mono} \cdot P_{ep} \cdot Acc \cdot VE} \right) \cdot \frac{1}{PE} \quad (11)$$

where P_{ep} is the epithelial membrane permeability coefficient, VE is the surface expansion ratio by the villi structure, and Acc is the accessibility of a drug to the epithelial membrane (Oliver et al., 1998). Since Acc has little effect on P_{eff} calculation (Sugano et al., 2009), Acc was set to 1 for simplification. In the present study, only undissociable compounds were used as model drugs. Therefore, P_{ep} is equal to intrinsic transcellular permeability and was roughly estimated from the octanol water partition coefficient ($\log P_{oct}$) ($\log P_{ep}$ (cm/s) = 1.1 $\log P_{oct}$ − 5.63) (Sugano, 2009a). The estimation errors of P_{ep} have little effect on P_{eff}, since P_{UWL} dominated Eq. (11) for the model compounds used in this study.

Table 1
Compound parameters.

	Griseofulvin	Efavirenz	Danazol	Cilostazol
MW	353	316	337	369
$\log P_{oct}$	2.5[a]	4.1[b]	4.5[a]	2.7[c]
S_0 (mg/mL)	0.010[d]	0.010[b]	0.0002[d,e]	0.0063[c,e]
$S_{dissolve}$ (mg/mL)	0.015[d]	0.194[b]	0.020[d,e]	0.0080 (fasted), 0.013 (fed)[c,e]
D_{mono} ($\times 10^{-6}$ cm^2/s)	7.3	7.7	7.4	7.1
P_{ep} (cm/s)	0.0013	0.076	0.21	0.0022

[a] Glomme et al. (2006).
[b] Takano et al. (2006).
[c] Jinno et al. (2006).
[d] Okazaki et al. (2008).
[e] Estimated from solubility in human FaSSIF (3 mM taurocholic acid (TC)/0.75 mM egg lecithin (EL)) and FeSSIF (15 mM TC/3 mM EL) for dog conditions (5 mM TC/1.25 mM EL and 15 mM TC/3 mM EL for the fasted and fed states, respectively).

2.3. Theoretical Fa calculation

Fa was calculated as previously reported (Sugano, 2009b, 2009c). To simplify the parameter optimization process, an analytical solution with a steady-state approximation was used to calculate *Fa*. In brief, the permeation number (*Pn*), the dose number (*Do*), and the dissolution number (*Dn*) were calculated as (Oh et al., 1993; Sugano, 2009c),

$$Pn = \frac{2DF}{R_{GI}} \cdot P_{eff} \cdot T_{si} \tag{12}$$

$$Do = \frac{Dose}{S_{dissolv} \cdot V_{GI}} \tag{13}$$

$$Dn = \frac{3 \cdot D_{eff,bulk} \cdot S_{dissolv}}{\rho} \cdot T_{si} \cdot \sum_i \frac{f_i}{r_{p,i}^2} \tag{14}$$

where $D_{eff,bulk}$ is the effective diffusion coefficient for dissolution in the bulk fluid which can be calculated in similar to $D_{eff,UWL}$. *Dn* was modified from the previous definition considering the particle size distribution. By using *Pn*, *Do* and *Dn*, *Fa* for low solubility compounds can be calculated as (Sugano, 2009c),

$$Fa = 1 - \exp\left(-\frac{1}{1/Dn + Do/Pn} \cdot Tn_{exss}\right) \tag{15}$$

When dissolution is quick, $1/Dn \ll Do/Pn$ and $Fa = X_{abs}/Dose \approx Pn/Do$ (cf. $1 - \exp(1-x) \approx x$, at $x < 0.7$). This equation is same as Eq. (1) divided by *Dose*. Drug parameters used for *Fa* calculation was summarized in Table 1. To reflect the residual particle effect (RPE) (Sugano, 2009a), a dimensionless number which express the prolonged duration of saturated concentration (Tn_{exss}) was introduced as (Sugano, 2009b),

$$Tn_{exss} = \frac{T_{sat}}{T_{si}} = 1 - \frac{1}{k_t \cdot T_{si}} \ln\left(\frac{1}{1 + DoDn/Pn}\right)$$
$$Do \cdot (1 - EXT(T_{exss})) > 1 \tag{16}$$

$$Tn_{exss} = 1 - \frac{1}{k_t \cdot T_{si}} \ln\left(\frac{1}{1 - 1/Do} - 1\right) \tag{17}$$

The smaller value of Eq. (16) or (17) should be taken as Tn_{exss}. Eq. (15) was found to give similar *Fa* values calculated by the dynamic compartmental model (<5% mean square root error) for a wide range of drug property (Sugano, 2009b).

2.4. Validation data set

Clinical *Fa* data of efavirenz (FDA approval document for Sustiva) and griseofulvin (Ahmed et al., 2008; Chiou and Riegelman, 1971) were used for validation. In addition, the dog *Fa* data of cilostazol (Jinno et al., 2006) and danazol (Liversidge and Cundy, 1995; Takano et al., 2008) were also used. These compounds were selected since these compounds are undissociable compounds (therefore, the effect of the stomach could be neglected) and particle size data were available in the literature. *Fa* was calculated from the PK data as previously reported by Takano et al. (2008, 2006) (Table 2).

2.5. Physiological and drug parameters

Following physiological parameters were used: $h_{totUWL} = 0.03$ cm, $h_{fam} = 0.0015$ cm, $V_{GI} = 3.6$ mL/kg, $DF = 1.7$ and $VE = 10$ (above for both humans and dogs), the body weight = 70

Table 2
Calculated and observed *Fa*.

Compound (species)	r_p (μm)	*Dose* (mg (mg/kg))	R_{SA}	h_{eff} (μm)	P_{eff} ($\times 10^{-4}$ cm/s)		$Fa\%_{calc}$			$Fa\%_{obs}$[a]
				+PDE	−PDE	+PDE	−PDE, −PRE	−PDE, +PRE	+PDE, +PRE	
Efavirenz (human, fasted)	1.5	600 (8.6)	2.1	82	1.4	3.4	28	40	70	82
	1.5	1200 (17)	4.2	49	1.4	5.2	15	24	64	59
Griseofulvin (human, fasted)	2	125 (1.8)	0.33	253	5.6	6.5	39	58	63	45
	2	500 (7.1)	1.3	122	5.6	12	12	22	43	43
Cilostazol (dog, fasted)	0.11	100 (10)	34	19	2.2	26	3	7	56	100
	1.2	100 (10)	3.1	61	2.2	9.1	3	7	25	21
	6.5	100 (10)	0.57	219	2.2	2.9	3	6	8	20
Cilostazol (dog, fed)	0.11	100 (10)	34	19	1.6	18	4	8	58	95
	1.2	100 (10)	3.1	61	1.6	6.6	4	8	27	75
	6.5	100 (10)	0.57	219	1.6	2.1	4	7	9	32
Danazol (dog, fasted)	0.085	200 (20)	87	17	0.5	4.1	1	2	15	77
	5	200 (20)	1.5	111	0.5	0.9	1	2	3	4.8
	2.5	20 (2.0)	0.30	258	0.5	0.5	8	14	15	12

[a] In vivo *Fa* data calculated as reported (Takano et al., 2006).

and 10 kg, $PE = 3$ and 1, $R_{GI} = 1.5$ and 0.5 cm, $T_{si} = 3.5$ and 2 h, $k_t = 1.3$ and 2.3 h^{-1} and $P_{WC} = 0.23 \times 10^{-4}$ and 0.29×10^{-4} cm/s (above for humans and dogs, respectively) (Sugano, 2009d and references therein). $D_{bm} = 1.1 \times 10^{-6}$ cm/s for dogs (both in the bulk fluid and UWL) and $D_{bm} = 0.12 \times 10^{-6}$ cm/s (in the bulk fluid) and $D_{bm} = 0.36 \times 10^{-6}$ cm/s (in the UWL) for humans (Okazaki et al., 2007; Sugano, 2009a; Sugano et al., 2007). The drug parameters are summarized in Table 1.

2.6. Optimization of C_{pd} and R_{fam}

The sum of root square error (*SSE*) was used as the target value to optimize C_{pd}.

$$SSE = \sum \sqrt{(observed\ \ Fa - theoretical\ \ Fa)^2} \quad (18)$$

All in vivo data were used for optimization assuming that C_{pd} was the same between humans and dogs. Minimum *SSE* was obtained using Excel solver function. Optimized C_{pd} was 1.3. Since only one fitting parameter was used, there would be no over-fitting.

3. Results and discussion

In the case of moderate dose strength and particles radius (*Dose* < ca. 4–5 mg/kg, r_p > ca. 3 μm), the theoretical framework of Eqs. (9)–(15) was found to be appropriate without considering the particle drifting effect (Sugano, 2009a,c, 2009d; Takano et al., 2006). However, as shown in Table 1 and Figs. 3–6, in the case of high dose and small particle size cases, calculation by the previous theory underestimated the experimental observation.

As discussed in Section 2, one possible reason for this discrepancy would be the effect of drug particles drifted into the UWL which was not taken into account previously. Considering the ample of experimental observations that micro-scale particles can exist in the UWL (Doyle-McCullough et al., 2007; Hodges et al., 1995; Limpanussorn et al., 1998; Norris et al., 1998; Smyth et al., 2008), the particle drifting effect should be taken into account. The particle drifting effect would become significant as the dose strength becomes higher and the particle size becomes smaller.

Since the self-diffusion of micro- and sub-micrometer scale particles is negligibly small, the drug particles may be drifted into the UWL by the fluctuating fluid flow and/or the sedimentation by gravity. Fluctuation of the intestinal fluid flow by the peristaltic moves of the intestinal wall is a well-known phenomenon. The loosely adhered mucus was known to be easily removed by a flow (Allen and Flemstroem, 2005; Atuma et al., 2001). Therefore, the UWL would not be a completely static water layer. The fluid in the UWL can be renewed by an occasional strong flow and drug particles can be carried into the UWL. However, the average flow in the UWL is

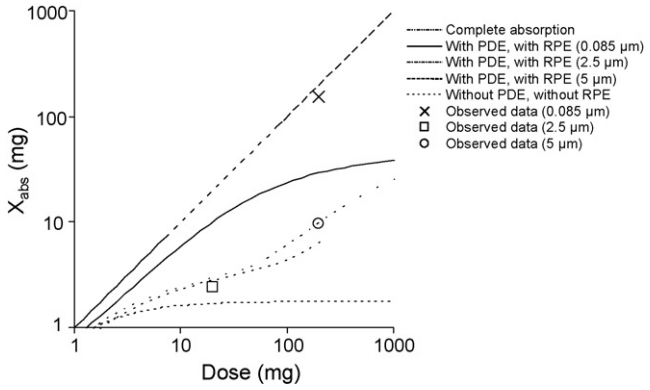

Fig. 5. Predicted vs observed X_{abs} of danazol in dogs.

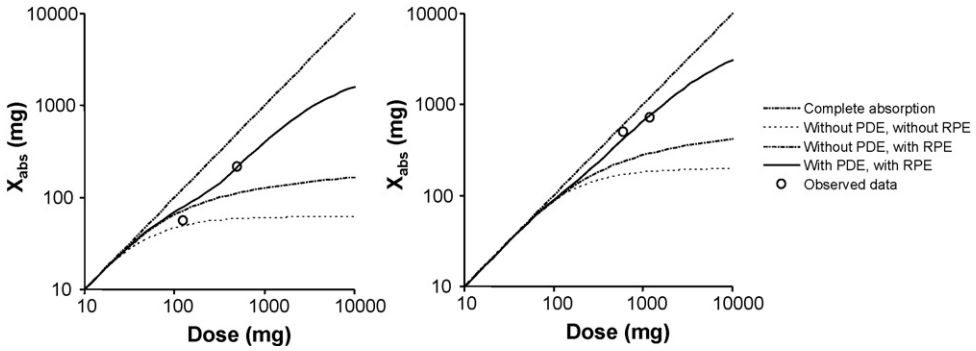

Fig. 3. Predicted vs observed X_{abs} in humans: (A) griseofulvin and (B) efavirenz.

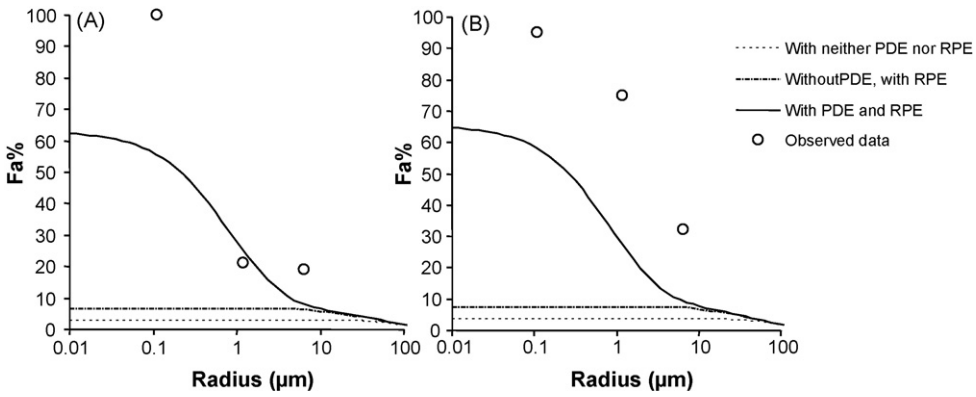

Fig. 4. Predicted vs observed *Fa* of cilostazol in dogs. (A) Fasted and (B) fed.

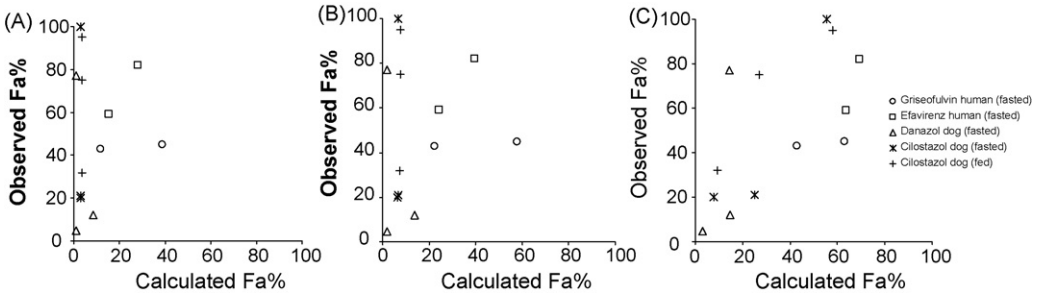

Fig. 6. Overall comparison of predicted vs observed *Fa*. (A) With neither RPE nor PDE, (B) with RPE, without PDE and (C) with both RPE and PDE.

weak and the UWL becomes a barrier against self-diffusion in the majority of a time.

By considering the particle drifting effect, the effects of both dose escalation and particle size reduction was more appropriately calculated for various compounds (Table 1 and Figs. 3–6).

The ratio of the total thickness of the GI fluid and UWL (f_{UWL}) was calculated to be ca. 0.2. Therefore, even in the absence of biased particle drifting toward the epithelial membrane, ca. one-fifth of the particles would exist within the UWL. In a fluctuating flow, floating particles can be carried by a flow to the place where the average flow is weak and sediment there (cf., snow drifting to the hedge or the sand drifting to the coast), resulting in a biased distribution between the bulk fluid and the UWL space. In addition, it was reported that the particles can exist in the villi interspaces, resulting in expansion of the accessible surface area (Doyle-McCullough et al., 2007; Norris et al., 1998). C_{pd} may reflect both the biased distribution and the possible expansion of the accessible surface area.

Fig. 7 shows the relationship between h_{eff}, *Dose* and particle diameter (=$2r_p$). It was suggested that when the dose (mg)/particle diameter (μm) ratio exceeds ca. 20, the particle drifting effect would become significant (h_{eff} < ca. 0.27).

However, there remained some deviations. These deviations may be due to the simple mathematical form of h_{eff} calculation, the dynamic change of h_{eff} and P_{eff} due to the absorption of drug, interaction with the mucus layer, etc. The concept of the particle drifting effect and the mathematical models proposed in the present study are the possible hypothesis, and further validation and improvement are required.

It is interesting that a significant increase of X_{abs} by nano-milled formulation was partly explained by the particle drifting effect. The penetration of nano-particles into the firmly adhered region and/or the increase of solubility (cf. Ostwald–Freundlich equation) would be a possible reason for the remaining discrepancy.

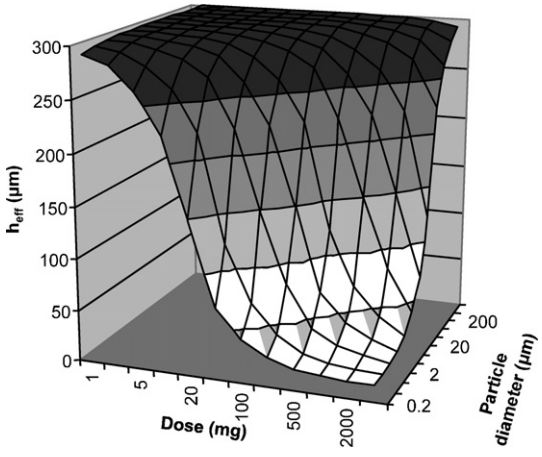

Fig. 7. Relationship between h_{eff}, dose and particle diameter.

The particle drifting effect would not be anticipated in the case of epithelial membrane limited permeation. This is in good agreement with that the saturation of oral absorption was more notably observed for the mid to low permeability drugs, such as pranlukast (Brocks et al., 1996; Yamashita et al., 2000) and chlorothiazide (Dressman et al., 1984).

In conclusion, in the present study, three reasons were raised to support the hypothesis of the particle drifting effect: (1) an underestimation of P_{eff} should be the reason for discrepancy between the previous theory and experimental observations (since the increase of solubility and the transit time was eliminated from the possible reason), (2) many reports suggested that micro-scale particles drifted into the UWL and even into the epithelial membrane, and (3) the mathematical model for the particle drifting effect introduced in this study appropriately depicted the effect of both dose escalation and particle size reduction.

References

Ahmed, I.S., Aboul-Einien, M.H., Mohamed, O.H., Farid, S.F., 2008. Relative bioavailability of griseofulvin lyophilized dry emulsion tablet vs. immediate release tablet: a single-dose, randomized, open-label, six-period, crossover study in healthy adult volunteers in the fasted and fed states. Eur. J. Pharm. Sci. 35, 219–225.

Allen, A., Flemstroem, G., 2005. Gastroduodenal mucus bicarbonate barrier: protection against acid and pepsin. Am. J. Physiol. 288, C1–C19.

Amidon, G.E., Higuchi, W.I., Ho, N.F.H., 1982. Theoretical and experimental studies of transport of micelle-solubilized solutes. J. Pharm. Sci. 71, 77–84.

Atuma, C., Strugala, V., Allen, A., Holm, L., 2001. The adherent gastrointestinal mucus gel layer: thickness and physical state in vivo. Am. J. Physiol. 280, G922–G929.

Avdeef, A., 2003. Absorption and Drug Development. Wiley-Interscience.

Avdeef, A., 2006. High-throughput solubility, permeability, and the MAD PAMPA model. In: Testa, B., Krämer, S., Wunderli-Allenspach, H., Folkers, G. (Eds.), Pharmacokinetic Profiling in Drug Research. Wiley-VCH, Zurich.

Brocks, D.R., Upward, J.W., Georgiou, P., Stelman, G., Doyle, E., Allen, E., Wyld, P., Dennis, M.J., 1996. The single and multiple dose pharmacokinetics of pranlukast in healthy volunteers. Eur. J. Clin. Pharmacol. 51, 303–308.

Chiou, W.L., Riegelman, S., 1971. Absorption characteristics of solid dispersed and micronized griseofulvin in man. J. Pharm. Sci. 60, 1376–1380.

Desai, M.P., Labhasetwar, V., Amidon, G.L., Levy, R.J., 1996. Gastrointestinal uptake of biodegradable microparticles: effect of particle size. Pharm. Res. 13, 1838–1845.

Doyle-McCullough, M., Smyth, S.H., Moyes, S.M., Carr, K.E., 2007. Factors influencing intestinal microparticle uptake in vivo. Int. J. Pharm. 335, 79–89.

Dressman, J.B., Amidon, G.L., Fleisher, D., 1985. Absorption potential: estimating the fraction absorbed for orally administered compounds. J. Pharm. Sci. 74, 588–589.

Dressman, J.B., Fleisher, D., 1986. Mixing-tank model for predicting dissolution rate control or oral absorption. J. Pharm. Sci. 75, 109–116.

Dressman, J.B., Fleisher, D., Amidon, G.L., 1984. Physicochemical model for dose-dependent drug absorption. J. Pharm. Sci. 73, 1274–1279.

Fagerholm, U., Lennernaes, H., 1995. Experimental estimation of the effective unstirred water layer thickness in the human jejunum, and its importance in oral drug absorption. Eur. J. Pharm. Sci. 3, 247–253.

Florence, A.T., 1997. The oral absorption of micro- and nanoparticulates: neither exceptional nor unusual. Pharm. Res. 14, 259–266.

Galia, E., Nicolaides, E., Horter, D., Lobenberg, R., Reppas, C., Dressman, J.B., 1998. Evaluation of various dissolution media for predicting in vivo performance of class I and II drugs. Pharm. Res. 15, 698–705.

Gaumet, M., Gurny, R., Delie, F., 2009. Localization and quantification of biodegradable particles in an intestinal cell model: the influence of particle size. Eur. J. Pharm. Sci. 36, 465–473.
Glomme, A., März, J., Dressman, J., 2006. Predicting the intestinal solubility of poorly soluble drugs. In: Testa, B., Krämer, S., Wunderli-Allenspach, H., Folkers, G. (Eds.), Pharmacokinetic Profiling in Drug Research. Wiley-VCH, Zurich, pp. 259–280.
Haruta, S., Iwasaki, N., Ogawara, K.-i., Higaki, K., Kimura, T., 1998. Absorption behavior of orally administered drugs in rats treated with propantheline. J. Pharm. Sci. 87, 1081–1085.
Hodges, G.M., Carr, E.A., Hazzard, R.A., Carr, K.E., 1995. Uptake and translocation of microparticles in small intestine. Morphology and quantification of particle distribution. Dig. Dis. Sci. 40, 967–975.
Jinno, J.-I., Kamada, N., Miyake, M., Yamada, K., Mukai, T., Odomi, M., Toguchi, H., Liversidge, G.G., Higaki, K., Kimura, T., 2006. Effect of particle size reduction on dissolution and oral absorption of a poorly water-soluble drug, cilostazol, in beagle dogs. J. Control. Release 111, 56–64.
Johnson, K.C., 2003. Dissolution and absorption modeling: model expansion to simulate the effects of precipitation, water absorption, longitudinally changing intestinal permeability, and controlled release on drug absorption. Drug Dev. Ind. Pharm. 29, 833–842.
Johnson, K.C., Swindell, A.C., 1996. Guidance in the setting of drug particle size specifications to minimize variability in absorption. Pharm. Res. 13, 1795–1798.
Lennernaes, H., 2007. Intestinal permeability and its relevance for absorption and elimination. Xenobiotica 37, 1015–1051.
Limpanussorn, J., Simon, L., Dayan, A.D., 1998. Transepithelial transport of large particles in rat: a new model for the quantitative study of particle uptake. J. Pharm. Pharmacol. 50, 753–760.
Liversidge, G.G., Cundy, K.C., 1995. Particle size reduction for improvement of oral bioavailability of hydrophobic drugs. I. Absolute oral bioavailability of nanocrystalline danazol in beagle dogs. Int. J. Pharm. 125, 91–97.
Martin, Y.C., 1981. A practitioner's perspective of the role of quantitative structure-activity analysis in medicinal chemistry. J. Med. Chem. 24, 229–237.
Moyes, S.M., Smyth, S.H., Shipman, A., Long, S., Morris, J.F., Carr, K.E., 2007. Parameters influencing intestinal epithelial permeability and microparticle uptake in vitro. Int. J. Pharm. 337, 133–141.
Norris, D.A., Puri, N., Sinko, P.J., 1998. The effect of physical barriers and properties on the oral absorption of particulates. Adv. Drug Deliv. Rev. 34, 135–154.
Obata, K., Sugano, K., Saitoh, R., Higashida, A., Nabuchi, Y., Machida, M., Aso, Y., 2005. Prediction of oral drug absorption in humans by theoretical passive absorption model. Int. J. Pharm. 293, 183–192.
Oh, D.M., Curl, R.L., Amidon, G.L., 1993. Estimating the fraction dose absorbed from suspensions of poorly soluble compounds in humans: a mathematical model. Pharm. Res. 10, 264–270.
Okazaki, A., Mano, T., Sugano, K., 2007. Theoretical dissolution model of polydisperse drug particles in biorelevant media. J. Pharm. Sci. Technol. Jpn. 67 (meeting abstract and poster).
Okazaki, A., Mano, T., Sugano, K., 2008. Theoretical dissolution model of polydisperse drug particles in biorelevant media. J. Pharm. Sci. 97, 1843–1852.
Oliver, R.E., Jones, A.F., Rowland, M., 1998. What surface of the intestinal epithelium is effectively available to permeating drugs? J. Pharm. Sci. 87, 634–639.
Sawamoto, T., Haruta, S., Kurosaki, Y., Higaki, K., Kimura, T., 1997. Prediction of the plasma concentration profiles of orally administered drugs in rats on the basis of gastrointestinal transit kinetics and absorbability. J. Pharm. Pharmacol. 49, 450–457.
Smyth, S.H., Feldhaus, S., Schumacher, U., Carr, K.E., 2008. Uptake of inert microparticles in normal and immune deficient mice. Int. J. Pharm. 346, 109–118.
Sugano, K., 2009a. Estimation of effective intestinal membrane permeability considering bile micelle solubilisation. Int. J. Pharm. 368, 116–122.
Sugano, K., 2009b. Fraction of dose absorbed calculation: comparison between analytical solution based on one compartment steady state approximation and dynamic seven compartment model. CBI J. 9, 75–93.
Sugano, K., 2009c. Introduction to computational oral absorption simulation. Expert. Opin. Drug Metab. Toxicol. 5, 259–293.
Sugano, K., 2009d. Oral absorption simulation for poor solubility compounds. Chem. Biodivers. 6, 2014–2029.
Sugano, K., 2009e. Theoretical investigation of passive intestinal membrane permeability using Monte Carlo method to generate drug-like molecule population. Int. J. Pharm. 373, 55–61.
Sugano, K., Cucurull-Sanchez, L., Bennett, J., 2009. Membrane permeability—measurement and prediction in drug discovery. In: Faller, B., Urban, L. (Eds.), Hit to Lead Optimization. Wiley-VCH, Weinheim, pp. 117–143.
Sugano, K., Okazaki, A., Sugimoto, S., Tavornvipas, S., Omura, A., Mano, T., 2007. Solubility and dissolution profile assessment in drug discovery. Drug Metab. Pharmacokinet. 22, 225–254.
Takano, R., Furumoto, K., Shiraki, K., Takata, N., Hayashi, Y., Aso, Y., Yamashita, S., 2008. Rate-limiting steps of oral absorption for poorly water-soluble drugs in dogs; prediction from a miniscale dissolution test and a physiologically-based computer simulation. Pharm. Res. 25, 2334–2344.
Takano, R., Sugano, K., Higashida, A., Hayashi, Y., Machida, M., Aso, Y., Yamashita, S., 2006. Oral absorption of poorly water-soluble drugs: computer simulation of fraction absorbed in humans from a miniscale dissolution test. Pharm. Res. 23, 1144–1156.
Yamashita, S., Furubayashi, T., Kataoka, M., Sakane, T., Sezaki, H., Tokuda, H., 2000. Optimized conditions for prediction of intestinal drug permeability using Caco-2 cells. Eur. J. Pharm. Sci. 10, 195–204.
Yu, L.X., 1999. An integrated model for determining causes of poor oral drug absorption. Pharm. Res. 16, 1883–1887.
Yu, L.X., Amidon, G.L., 1998. Characterization of small intestinal transit time distribution in humans. Int. J. Pharm. 171, 157–163.
Yu, L.X., Amidon, G.L., 1999. A compartmental absorption and transit model for estimating oral drug absorption. Int. J. Pharm. 186, 119–125.